Available online at www.sciencedirect.com
ScienceDirect
Journal of Nuclear Materials 357 (2006) 213–220
journal of nuclear materials
www.elsevier.com/locate/jnucmat

An analytical model for the Amoeba effect in UO_2 fuel pellets

Yong Choi [a], Jong K. Lee [b,*]

[a] Department of Electronic Materials, Sun Moon University, Asan-City, Chung-Nam 336-840, Republic of Korea
[b] Department of Materials Science and Engineering, Michigan Technological University, Houghton, MI 49931, USA

Received 10 April 2006; accepted 30 May 2006

Abstract

Significant temperature gradients are present across the fuel particles when a nuclear reactor is producing power. If local temperatures are sufficiently high, nuclear fuel kernels can migrate up the thermal gradient. During this process, the barrier retaining fission product is progressively damaged, and the damage can lead to complete failure of the coating system. This phenomenon is called the Amoeba effect. In this model, the Amoeba effect is analyzed in terms of an interactive transport phenomenon between the solid-state diffusion of oxygen ions in a UO_2 kernel and the flow of CO gas molecules through the pyrocarbon buffer layer surrounding the kernel. For mathematical simplicity, a cylindrically-shaped kernel is assumed. The results show that not only a concentration gradient in oxygen ions but also a temperature gradient with a negative heat of transport for oxygen ions can cause the Amoeba effect in UO_2 fuel particles.

1. Introduction

Recently, high temperature gas cooled reactors (HTGR) have attracted much attention for hydrogen production through the use of nuclear power [1,2]. In a HTGR, a coated nuclear particle is made of a spherical uranium oxide (or carbide) kernel typically encased with a buffer and an inner pyrolytic carbon layer, a silicon carbide (SiC) layer, and an outer pyrolytic carbon layer [3]. Significant temperature gradients can be present across the fuel particles when a nuclear reactor is producing power. If local temperatures are sufficiently high, the fuel kernels can migrate up the thermal gradient. During this process, the pyrocarbon and SiC layers retaining fission product are progressively damaged, leading to complete failure of the coating system. This phenomenon is called *Amoeba effect* [4–7]. It has been encountered in uranium, thorium, and plutonium fuels in the oxide or carbide form. For carbide fuels, migration is caused by solid-state diffusion of carbon to the cooler side of the kernel. For oxide kernels, migration may be caused by CO gas diffusion, solid-state diffusion of oxygen to the hotter side, solid-state diffusion of carbon, or any combination of them. In this work, we present a model to examine the Amoeba effect in UO_2 fuel, assuming that it is caused by an interactive transport between CO gas flow and diffusion of oxygen ions.

It appears that Gulden [4] and Wagner-Löffler [6] were the first to put forward a theory on the Amoeba

* Corresponding author. Tel.: +1 906 487 2266; fax: +1 906 487 2934.
E-mail address: jkl103@mtu.edu (J.K. Lee).

0022-3115/$ - see front matter © 2006 Elsevier B.V. All rights reserved.
doi:10.1016/j.jnucmat.2006.05.053

Nomenclature

$C_{[O]}$	concentration of oxygen ions in mass per unit volume
$C^{c}_{[O]}$	concentration of oxygen ions at the cold side
$C^{h}_{[O]}$	concentration of oxygen ions at the hot side
$\nabla C_{[O]}$	oxygen concentration gradient
d	average diameter of carbon particles in the buffer PyC
$D_{[O]}$	diffusion coefficient of oxygen ions
η	viscosity of CO gas
$J_{[O]}$	oxygen flux through the kernel
k_c	forward rate constant due to $C^{c}_{[O]}$
k_h	forward rate constant due to $C^{h}_{[O]}$
L_b	diameter and length of the cylindrical buffer PyC
L_k	diameter and length of the cylindrical kernel
m_C	atomic weight of carbon
m_{CO}	molecular weight of CO
m_O	atomic weight of oxygen ion
$\dot{M}$	mass flow rate of CO through the annulus
$\dot{M}_c$	rate of CO formation at the cold end of the kernel
$\dot{M}_h$:	rate of CO formation at the hot end of the kernel
$\mu_{[O]}$	chemical potential of oxygen ion
p_m	permeability factor for CO gas molecules in the annulus
$\overline{P}$	average CO pressure equal to $(P^{h}_{CO} + P^{c}_{CO})/2$
P^{c}_{CO}	partial vapor pressure of CO at the cold side
P^{h}_{CO}	partial vapor pressure of CO at the hot side
ΔP	pressure drop equal to $P^{h}_{CO} - P^{c}_{CO}$
q_c	backward rate constant due to P^{c}_{CO}
q_h	backward rate constant due to P^{h}_{CO}
$Q^{*}_{[O]}$	heat of transport for oxygen ions in UO_2
R	the gas constant, 8.3144 J/mole-K
r_b	outer radius of a spherical buffer PyC shell
r_k	radius of a spherical UO_2 kernel
ρ_C	density of buffer PyC
$\overline{T}$	average temperature of the kernel equal to $(T_h + T_c)/2$
∇T	temperature gradient in the kernel
v_s	superficial average velocity of CO gas molecules
v_{CO}	molar volume of CO gas
$\dot{V}$	volume flow rate of CO through the annulus
ω	void fraction in the buffer PyC layer
Ω_C	*effective* volume of carbon per unit mass
$\dot{x}$	migration rate of the kernel

effect. In Wagner-Löffler's classic work [6], the kernel migration rate was given in terms of the product of the temperature gradient and the heat of transport for oxygen ions, and an interesting montage was presented to link the various relationships among redox reactions and diffusion steps. In the work, however, the contribution due to the concentration gradient in oxygen ions was not considered. Furthermore, the model did not treat the interplaying relationship between the oxygen diffusion within the kernel and the CO gas flow through the buffer pyrolytic carbon layer surrounding the kernel. In this study, an analytical model is presented to take into account for both the oxygen concentration gradient effect and the relationship between oxygen diffusion and CO gas flow. For mathematical simplicity, a cylindrical geometry, instead of a spherical one, for the fuel particle is adopted since an annulus shell with a constant cross section area permits an analysis for CO gas flow through the packed bed of carbon clusters in the buffer pyrolytic carbon layer.

2. Analyses

Typically, UO_2 kernels are processed in spherical shapes with radii equal to about 100–300 μm. The kernels are then embedded in a multi-shell structure made of a buffer pyrolytic carbon (PyC) layer of 100 μm thick and three more layers of PyC and SiC. For mathematical simplicity, however, we will assume a cylindrically-shaped pellet instead of a spherical pellet geometry, as schematically shown in Fig. 1. The layers of inner PyC, SiC, and outer PyC are not drawn. A pellet is here termed to indicate the structure combining both the UO_2 kernel and its outer shells. At a constant volume con-

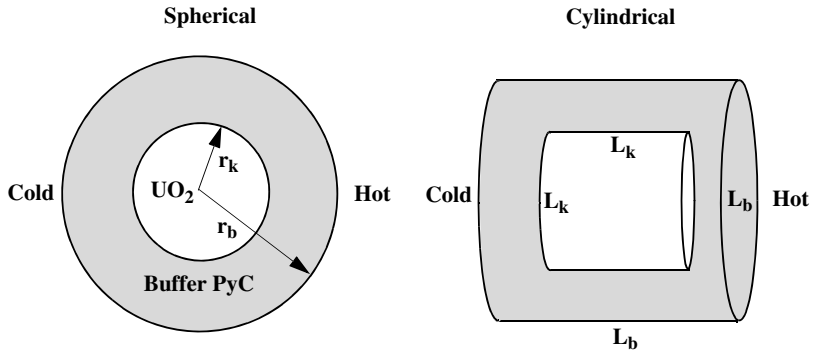

	r	L
kernel	200 μm	349 μm
buffer	300 μm	524 μm

Fig. 1. Schematics of a UO_2 pellet structure. A cylindrical configuration is used for gas flow analysis in the buffer PyC layer. r_k is the radius of a spherical kernel, and L is the height and the diameter of a cylindrical body.

dition, a set of appropriate dimensions is compared in the figure: r is the radius of a spherical frame and L is the height and the diameter of a cylindrical body. As it will be shown later, an advantage of a cylindrical geometry is that, without losing main features of physics involved, it allows a simple analysis for a gas flow through the buffer PyC layer.

2.1. Oxygen diffusion in a kernel

Let us consider the migration rate of the kernel at a steady state, $\dot{x}$. In terms of $J_{[O]}$, the oxygen flux through the kernel, and Ω_C, the *effective* volume of carbon per unit mass, the migration rate is given by

$$\dot{x} = J_{[O]}\Omega_C. \tag{1}$$

The cold end of the kernel is set at $x = 0$ and the hot end is at $x = L_k$, see Fig. 2. From diffusion theory [8]

$$J_{[O]} = -D_{[O]}\left[\nabla C_{[O]} + \frac{C_{[O]}Q^*_{[O]}\nabla T}{RT^2}\right], \tag{2}$$

where $D_{[O]}$ is the diffusion coefficient, $C_{[O]}$ is the concentration, and $Q^*_{[O]}$ is the heat of transport, all for oxygen ions in a UO_2 kernel. $\nabla C_{[O]}$ and ∇T are the gradients of the oxygen concentration and the temperature in the kernel, respectively. Thus, the kernel migration rate becomes

$$\dot{x} = -D_{[O]}\Omega_C\left[\nabla C_{[O]} + \frac{C_{[O]}Q^*_{[O]}\nabla T}{RT^2}\right]. \tag{3}$$

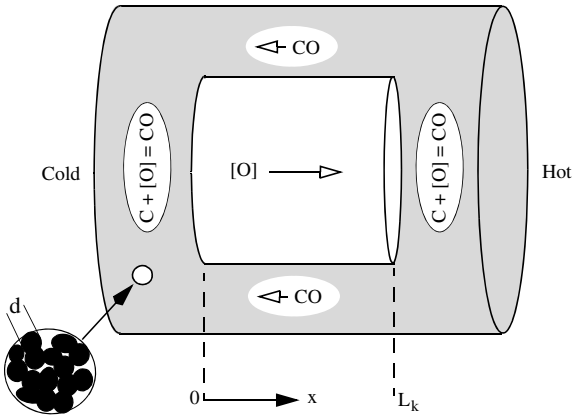

Fig. 2. Schematic for an annulus flow model. At the hot side, oxidation reaction produces CO, which flows down to the cold side through the buffer PyC. At the cold side, CO reduces to C and [O], and the oxygen ions, [O], transport to the hot side through diffusion in UO_2. The buffer PyC is made of carbon clusters with an average diameter equal to d.

Clearly, the sum of the gradient terms should be negative in order to provide a positive migration rate, i.e., a displacement of the kernel toward the hot side.

2.2. Carbon oxidation

For the kernel to migrate toward the hot side, some of carbons at the hot end of the buffer PyC must be consumed away through oxidation, as shown in Fig. 2. Therefore, a reaction at the kernel hot front is given by

$$C + [O] = CO. \tag{4}$$

Alternatively, the oxidation reaction can be considered in the form of CO_2 formation or a combination of both CO and CO_2, but no essential features will be lost with the treatment of CO alone. The rate of formation for CO may be written as

$$\dot{M}_h = k_h C^h_{[O]} - q_h P^h_{CO}, \tag{5}$$

where k_h is the forward rate constant, q_h the backward rate constant, $C^h_{[O]}$ the concentration of oxygen ions at the hot side, and P^h_{CO} is the partial vapor pressure of CO at the hot side. An implicit assumption of Eq. (5) is that there are always plenty of *activated* carbon atoms, and thus they do not control the oxidation reaction. Since the oxygen adions at the surface of the kernel are presumed to react with the carbon atoms in the buffer PyC, the surface concentration of oxygen ions should be used in Eq. (5). However, if the difference in chemical potential between the oxygen adions and the lattice oxygen ions within a UO_2 kernel is ignored, use of $C^h_{[O]}$ should be reasonable. A CaF_2-type UO_2 structure has two (400) planes made of oxygen ions [9], and the surface concentration becomes equal to the bulk concentration multiplied by one half of the lattice parameter of the unit cell.

Similarly, there also occurs redox reaction of carbon atoms (oxidation or reduction of CO) at the cold side, and the rate of formation for CO is given by

$$\dot{M}_c = k_c C^c_{[O]} - q_c P^c_{CO}. \tag{6}$$

For simplicity, redox reactions on the lateral surface of the cylindrical kernel are neglected: It could be reasoned that the CO gas produced at the upper half (hotter) of the lateral surface is reduced at the lower half (colder). It is clear that for the kernel to move from the cold to the hot side, $\dot{M}_h > \dot{M}_c$.

2.3. CO flow through the annulus

With $\dot{M}_h > \dot{M}_c$, the CO pressure is greater at the hot side than at the cold side. Thus, CO molecules flow down through the annulus filled with buffer PyC. According to a theory of fluid flow through packed beds [10], the *superficial* average velocity, v_s, for the CO gas molecules is given as

$$v_s = \frac{\Delta P}{L_k}\frac{(L_b/2)^2}{8\eta}\left[\frac{1-a^4}{1-a^2} + \frac{1-a^2}{\ln a}\right] p_m, \tag{7}$$

where $a = L_k/L_b$, η is the viscosity of CO gas, $\Delta P = P^h_{CO} - P^c_{CO}$, and p_m is a permeability factor accounting for the drag due to bedded carbon clusters in the buffer PyC. If the value of a approaches 0, Eq. (7) represents a Hagen–Poiseuille laminar flow [10], which should be reasonable with a low ΔP.

The permeability factor, p_m, may be approximated by

$$p_m = \frac{\omega^3 d^2}{20(1-\omega)^2 (L_b/2)^2}, \tag{8}$$

where ω is the void fraction and d is the average diameter of carbon particles in the buffer PyC [10]. The volume flow rate of CO through the annulus is then

$$\dot{V} = v_s \omega \pi (L_b/2)^2 (1-a^2) \tag{9}$$

and the corresponding mass flow rate of CO gas, $\dot{M}$, in the annulus is given by

$$\dot{M} = \dot{V} m_{CO}/v_{CO}, \tag{10}$$

where m_{CO} and v_{CO} are the molecular weight and molar volume of CO, respectively. Substituting Eqs. (7)–(9) into Eq. (10), we obtain

$$\dot{M} = \frac{\Delta P (L_b/2)^2}{L_k v_{CO}} \frac{\pi m_{CO} \omega^4 d^2 (1-a^2)}{160\eta(1-\omega)^2}\left[\frac{1-a^4}{1-a^2} + \frac{1-a^2}{\ln a}\right] = \alpha \frac{\Delta P (L_b/2)^2}{L_k v_{CO}}, \tag{11}$$

where

$$\alpha = \frac{\pi m_{CO} \omega^4 d^2 (1-a^2)}{160\eta(1-\omega)^2}\left[\frac{1-a^4}{1-a^2} + \frac{1-a^2}{\ln a}\right]. \tag{12}$$

With $m_{CO} = 28 \times 10^{-3}$ kg/mole, $\omega = 0.5$, $a = L_k/L_b = 349/524 = 0.67$, $d = 5$ nm, and $\eta = 2 \times 10^{-5}$ Pa s, $\alpha = 7.13 \times 10^{-18}$ m^3 s/mole. $\omega = 0.5$ is estimated from the difference in density between buffer PyC (1100 kg/m^3) and graphite (2267 kg/m^3). The density of the buffer PyC changes with the fission reaction in the pellet, and the viscosity of CO gas is a function of temperature. However, their changes are neglected. The molar volume of CO gas, v_{CO}, depends sensitively on the temperature and is left as a variable.

2.4. Steady state and rate constants

At a steady state, the CO flow rate through the annulus should be equal to the CO oxidation rate at the hot side, and also to the CO reduction rate at the cold side. Thus, we have

$$\dot{M} = \dot{M}_h = -\dot{M}_c \tag{13}$$

or

$$\alpha\frac{\Delta P(L_b/2)^2}{L_k v_{CO}} = k_h C^h_{[O]} - q_h P^h_{CO}. \quad (14)$$

The CO flow rate through the annulus is also related to the oxygen flux in the kernel as follows:

$$\dot{M} m_O/m_{CO} = J_{[O]} \cdot \text{Cross section area of the kernel} = J_{[O]}\pi(L_k/2)^2,$$

where m_O is the atomic weight of oxygen. Using Eqs. (2) and (14) and rearranging the above

$$J_{[O]} = \frac{\alpha\Delta P m_O}{\pi m_{CO} a^2 L_k v_{CO}}. \quad (15)$$

The *effective* volume of carbon per unit mass, Ω_C, in Eq. (1) is the volume of the carbon atoms in the buffer PyC, which *actually* react with the oxygen ions, and thus it is not simply equal to the inverse of the buffer PyC density, ρ_C. We note that the number of oxygen ions available for carbon oxidation are equal to $J_{[O]}N_{av}/m_O$ per unit area and per unit time, where N_{av} is Avogadro's number. Therefore, Ω_C is estimated to be

$$\Omega_C = m_C/(m_O\rho_C).$$

Finally, the expression for the kernel displacement rate, $\dot{x}$, becomes

$$\dot{x} = \frac{\alpha m_C \overline{P}\Delta P}{\pi m_{CO} a^2 L_k R\overline{T}\rho_C}, \quad (16)$$

where, assuming an ideal gas for CO, v_{CO} is equal to $R\overline{T}/\overline{P}$, R the gas constant, $\overline{T}$ the average temperature of the kernel, and $\overline{P}$ is the average CO pressure, i.e., $(P^h_{CO} + P^c_{CO})/2$. Eq. (16) can also be derived from the carbon consumption rate at the hot front of the kernel.

3. Results and discussion

In Fig. 3, the pressure drop ratio, $\Delta P/\overline{P}$, of the CO gas is plotted as a function of the average CO pressure, $\overline{P}$, which is necessary for a typical, steady-state kernel displacement rate, $\dot{x} = 1.4\times 10^{-5}$ μm/s [6], at the average kernel temperature, $\overline{T} = 1783$ K. We note that the pressure drop ratio requires several percentages at low burnup pressures of ~1 MPa, but much less at high burnup pressures of ~10 MPa. Although there has been much discussion, in the literature, on the release of fission gases and CO gas from UO_2 kernels [11], information on the partial vapor pressure of CO gas appears not

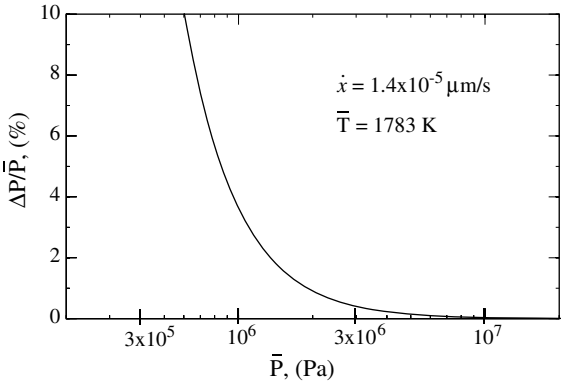

Fig. 3. A plot of $\Delta P/\overline{P}$ versus $\overline{P}$ at $\overline{T} = 1783$ K. For the plot, $\dot{x}$ is set at 1.4×10^{-5} μm/s. Note that the pressure drop ratio requires several percentages at low burnup pressures of $\sim10^6$ Pa, but insignificant percentages at high burnup pressures of $\sim10^7$ Pa.

available. Thus, for the plot, from low burnup pressures of ~1 MPa up to high burnup pressures of ~10 MPa are used. At $\overline{P} = 1$ MPa, the results show that about 4% of a pressure drop between the hot and the cold side is necessary to cause a kernel migration rate of 1.4×10^{-5} μm/s, whereas a much small difference can induce a kernel migration at $\overline{P} = 10$ MPa. Considering a crushing stress of ~100 MPa for UO_2 pellets under compression [11], the use of $\overline{P} = 1$ MPa seems reasonable.

Experimental information on the rate constants, k_h, k_c, q_h, and q_c, which appear in Eqs. (5) and (6), is hardly available. Thus, only a qualitative nature on their relationships is presented here. For the cold end, the UO_2 kernel is assumed to be a perfect crystal maintaining its stoichiometry, yielding $C_{[O]} = 1298$ kg/m^3 for the oxygen concentration [9]. Furthermore, $k_c = 2\times10^{-16}$ m^3/s and $q_c = 2.67\times10$ m s are assumed, for an illustrative purpose, for the kernel cold end. To maintain $\dot{x} = 1.4\times10^{-5}$ μm/s at $\overline{T} = 1783$ K and $\overline{P} = 1$ MPa, the necessary ratio of q_h/q_c is plotted as a function of the k_h/k_c ratio in Fig. 4. Clearly, with a different set of k_c and q_c values, the relationship should change. The equality relationship, $\dot{M} = \dot{M}_h = -\dot{M}_c$ of Eq. (13), is somewhat a restrictive one, although it conveniently provides mass conservation. If we view diffusion of CO gas molecules out of the kernel zone, $\dot{M}$ could be set equal to $\dot{M}_h - \dot{M}_c$, while allowing CO production at both the hot and cold ends through oxidation.

Interesting features are the amount of the oxygen concentration gradient, $\nabla C_{[O]}$, and the heat of oxygen transport, $Q^*_{[O]}$, appeared in Eq. (3). The

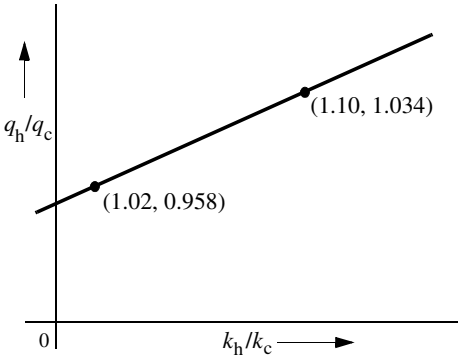

Fig. 4. Relationship between the rate constant ratios to sustain $\dot{x} = 1.4 \times 10^{-5}$ μm/s at $\overline{T} = 1783$ K and $\overline{P} = 1$ MPa.

diffusion coefficient of oxygen ions is sensitive on the stoichiometry of a uranium oxide crystal [9]. For example, $D_{[O]}$ is equal to 1.37×10^{-12} m^2/s for a stoichiometric crystal, $UO_{2.0}$, but an oxygen-deficient crystal, $UO_{1.9}$, shows a 59-fold increased value, 8.11×10^{-11} m^2/s at 1783 K. Similarly, an oxygen-rich crystal, $UO_{2.1}$, displays a high value, 6.58×10^{-11} m^2/s, suggesting the critical role of both oxygen interstitials and oxygen vacancies on diffusion. In Fig. 5, the values of $\nabla C_{[O]}$ and $Q^*_{[O]}$, necessary for $\dot{x} = 1.4 \times 10^{-5}$ μm/s at $T = 1783$ K with $\nabla T = 10^5$ K/m, are plotted for two different $D_{[O]}$ cases: The solid line is for the stoichiometric crystal, $UO_{2.0}$, and the dotted line is for the oxygen-deficient crystal, $UO_{1.9}$. In the absence of a thermal-transport with $Q^*_{[O]} = 0$, the $\nabla C_{[O]}$ value necessary for the same

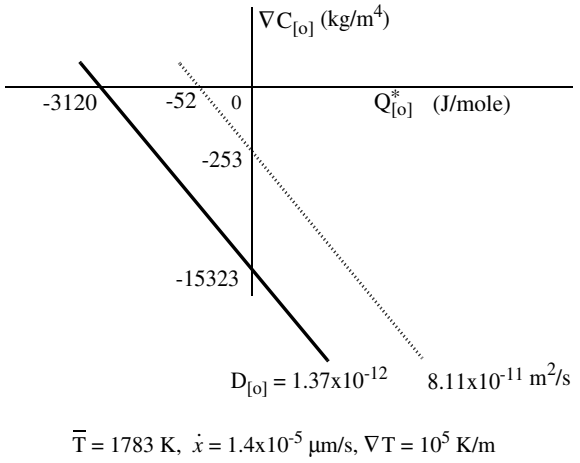

Fig. 5. $\nabla C_{[O]}$ versus $Q^*_{[O]}$ necessary for $\dot{x} = 1.4 \times 10^{-5}$ μm/s at $\overline{T} = 1783$ K with $\nabla T = 10^5$ K/m. The solid line is for the case with $D_{[O]} = 1.37 \times 10^{-12}$ m^2/s, and the dotted line is for the case with $D_{[O]} = 8.11 \times 10^{-11}$ m^2/s.

migration rate is equal to $-15\,323$ kg/m^4 for the stoichiometric case. This concentration gradient, $-15\,323$ kg/m^4, can be easily accomplished with a difference of only 0.4% in the oxygen vacancy concentration (or oxygen interstitial concentration) along the length of the kernel. Of course, with a higher oxygen diffusivity, the difference becomes less.

Even with $\nabla C_{[O]} = 0$, a negative heat of oxygen transport, $Q^*_{[O]}$, can induce migration of a kernel under a thermal gradient. For a stoichiometric case, the required $Q^*_{[O]}$ is -3120 J/mole as shown in Fig. 5. Heat of transport, Q^*, has been a subject of extensive investigation in the transport theory [8,12–14]. Briefly, it is the amount of heat flow resulting from the unit flow of jumping ions or atoms. If $Q^* > 0$, the jumping ions take heat along with them, and thus they tend to move toward the cold side in order to reduce the existing temperature gradient, i.e., in accordance with the second law of thermodynamics. If $Q^* < 0$, however, the ions are favoured to jump toward the hot end, again in order to curb the temperature gradient. The concept of a negative heat of transport can be understood with the following thought experiment. Let us imagine that the low temperature UO_2 structure (a CaF_2-type) undergoes a phase transition to a high temperature structure, say a rutile TiO_2-type, at $T = T_{tr}$. Further, we assume that the transition is accomplished mainly through the rearrangement of oxygen ions. If so, the chemical potential of oxygen ion may be approximated by

$$\mu_{[O]} = \mu^0_{[O]} + \Delta H_{tr}(1 - T/T_{tr}), \tag{17}$$

where $\mu^0_{[O]}$ is the free energy at a reference state, and ΔH_{tr} is the enthalpy change for the phase transition on heating.

In Eq. (17), T is assumed to be near T_{tr} and the enthalpy of uranium ions is assumed to be continuous across T_{tr} on the promise that the phase transition is mainly due to the rearrangement of oxygen ions. Now let us envision that a temperature gradient is imposed along a UO_2 bar – with $T_1 < T_{tr}$ at one end and $T_2 > T_{tr}$ at the other end of the bar. Because of the gradient in the chemical potential, there will be a flow of oxygen ions, whose flux is given by [8]

$$\begin{aligned} J_{[O]} &= -D_{[O]}C_{[O]}\nabla\mu_{[O]}/RT \\ &= -D_{[O]}C_{[O]}\{-\Delta H_{tr}/T_{tr}\}\nabla T/RT. \end{aligned} \tag{18}$$

Comparing Eqs. (2) to (18), we find $Q^*_{[O]} = -\Delta H_{tr}$. Since ΔH_{tr} is positive, $Q^*_{[O]}$ becomes negative in this fictitious experiment.

As for $Q^*_{[O]}$, Kamata and Esaka [12] presented about -10^5 J/mole for stoichiometric oxides of mixed uranium and plutonium $(Pu,U)O_2$. It is a large number, close to ten times the heat of fusion for most metals. Indeed Janek and Korte [13] questioned its validity due to the doubtful designs of thermal diffusion experiments on which the data was based. In a later work, Janek and Timm [14] discussed that $Q^*_{[O]}$ may depend sensitively on the ratio of oxygen interstitial mobility to oxygen vacancy mobility, ψ. According to their theory, $Q^*_{[O]}$, can range from -5×10^4 at $\psi = 0.5$ to $+5\times10^4$ J/mole at $\psi = 2$ for stoichiometric oxides. However, in view of uncertainties in the mobility values of both point defects, Janek and Timm's result is hardly applicable for elucidating the heat of transport in uranium oxides. Certainly, more information on $Q^*_{[O]}$ and other physical quantities such as CO pressure are needed to better quantify the Amoeba effect.

How practical is the use of a cylindrical geometry for a spherical fuel pellet? As noted before, a cylindrical annulus provides a constant cross section area for CO gas flow analysis (Eqs. (7) and (11)), whereas a spherical shell with its varying cross section does not. A gas flow analysis through a spherical shell would require a numerical modeling. Nevertheless, an estimation can be made on the base of the *effective* hot surface area for a spherical kernel. The current cylindrical geometry is equivalent to 0.76π for the solid angle of the effective hot spherical surface area or to a spherical cap with 52° as the cap angle. On the other hand, if we take 45° as the cap angle, the gas flow rate of Eq. (7) should be reduced by a factor of 1.3 $(=(1-\cos 52°)/(1-\cos 45°))$.

So far, the model has been addressed for the Amoeba effect in uranium oxide particles, where oxygen ions undergo uphill diffusion along the temperature gradient. For either UCO or UC_2 carbide fuels, however, migration is understood to occur by carbon diffusion *down* the temperature gradient [4,6]. The basic formulation of the current model should be applicable for a carbide case, provided that the oxygen ions are replaced with carbon atoms in Eq. (2), and the carbon redox reaction is treated as the principal contribution to the kernel migration. As briefly mentioned in Section 2.2, the role of CO_2 should be considered in the redox reaction of $2CO = CO_2 + C$.

The work of Bullock and Kaae [15] clearly demonstrated that carbon atoms build up at the cold side of a UO_2 kernel but also fill up fission-produced gas bubble voids within the kernel. The carbon-filled voids suggest not only the diffusion of carbon atoms but also the flow and decomposition of CO or CO_2 gas molecules within the kernel. During irradiation, kernels swell owing to solid fission product production and fission gas bubble formation. Concurrently, new point defects such as oxygen interstitials are produced, possibly at the expense of some old defects, leading to new defect equilibria both within and without the kernel. As a consequence, the size and the shape of a kernel change with irradiation, and the buffer PyC layer becomes compressed with an increase in its density. Therefore, the current model is valid only at the early stage of irradiation when the kernel swelling and fission gas production are negligible. One way to prevent kernel migration is, as the model suggests, to eliminate the flow of CO or CO_2 gas molecules down the temperature gradient and the diffusion of oxygen ions up the temperature gradient. In this sense, Bullock and Kaae's work [15] on the use of ZrC layer as an oxygen getter is consistent with the current understanding for the mechanism of the Amoeba effect. Clearly, further investigations, including numerical computations accounting for dimensional changes in a kernel during fissioning, are necessary to better understand the Amoeba effect in HTGR.

4. Conclusion

By adopting a cylindrical geometry in place of a spherical one for a uranium oxide kernel, the Amoeba effect is examined with a model which accounts for the relationship between the oxygen diffusion within the kernel and the CO gas flow through the buffer pyrolytic carbon layer surrounding the kernel. The results show that not only a concentration gradient in oxygen ions but also a temperature gradient with a negative heat of transport for oxygen ions can cause the Amoeba effect in UO_2 fuel particles: For example, either a 0.4% difference in the oxygen vacancy concentration along the length of the kernel or a heat of transport in the amount of -3120 J/mole alone can cause a typical kernel migration rate of 1.4×10^{-5} μm/s at 1783 K. A detailed quantitative test of the model, however, requires information on several ancillary physical data such as reaction rate constants and the vapor pressure of CO gas within fuel pellets. Finally, with a little change, the model can be applicable to the Amoeba problem occurring in nuclear carbide particles such as UCO.

Acknowledgements

The authors are indebted to the reviewer who kindly brought attention to the interesting work of R.E. Bullock and J.L. Kaae [15]. The work was financially supported by both Korea Institute of Science and Technology Evaluation and Planning (KISTEP) and the Ministry of Science and Technology (MOST) of Korea. The authors also thank Dr Y.W. Lee at Korea Atomic Energy Research Institute (KAERI), who provided valuable discussion and support during the course of the work.

References

[1] J.A. Lake, R.R. Schultz, DOE Advanced Reactor Research, INEEL, October 2003.
[2] IAEA-TECDOC–1085. Available from: <www.iaea.org/programmes/inis/aws/htgr/abstracts_c/abst_30027279.html>.
[3] D.A. Petti, DOE Advanced Gas Reactor Fuel Development and Qualification Program, INL, February 2005.
[4] T.D. Gulden, J. Am. Ceram. 55 (1972) 14.
[5] K. Iwamoto, S. Kashimura, A. Kikuchi, J. Nucl. Sci. Technol. 9 (1972) 465.
[6] M. Wagner-Löffler, Nucl. Technol. 35 (1977) 392.
[7] D.A. Petti, J. Buongiorno, J.T. Maki, R.R. Hobbins, G.K. Miller, Nucl. Eng. Des. 222 (2003) 281.
[8] P.G. Shewmon, Diffusion in Solids, 2nd Ed., TMS, Warrendale, PA, 1989.
[9] R.W. Cahn, P. Haasen, E.J. Kramer (Eds.), Materials Science and Technology – A Comprehensive Treatment, vol. 10A, Wiley, Weinheim, NY, 1991.
[10] D.R. Gaskell, An Introduction to Transport Phenomena in Materials Engineering, Mac-Millan, New York, NY, 1992.
[11] K. Sawa, K. Minato, J. Nucl. Sci. Technol. 36 (1999) 781.
[12] M. Kamata, T. Esaka, J. Appl. Electrochem. 24 (1994) 390.
[13] J. Janek, C. Korte, Z. Phys. Chem. 196 (1996) 187.
[14] J. Janek, H. Timm, J. Nucl. Mater. 255 (1998) 116.
[15] R.E. Bullock, J.L. Kaae, J. Nucl. Mater. 115 (1983) 69.